LETTERS
https://doi.org/10.1038/s41564-018-0223-6
nature microbiology

Inducible developmental reprogramming redefines commitment to sexual development in the malaria parasite *Plasmodium berghei*

Robyn S. Kent[1,2,5], Katarzyna K. Modrzynska[1,3,5*], Rachael Cameron[1], Nisha Philip[1,4], Oliver Billker[3*] and Andrew P. Waters[1*]

During malaria infection, *Plasmodium* spp. parasites cyclically invade red blood cells and can follow two different developmental pathways. They can either replicate asexually to sustain the infection, or differentiate into gametocytes, the sexual stage that can be taken up by mosquitoes, ultimately leading to disease transmission. Despite its importance for malaria control, the process of gametocytogenesis remains poorly understood, partially due to the difficulty of generating high numbers of sexually committed parasites in laboratory conditions[1]. Recently, an apicomplexa-specific transcription factor (AP2-G) was identified as necessary for gametocyte production in multiple *Plasmodium* species[2,3], and suggested to be an epigenetically regulated master switch that initiates gametocytogenesis[4,5]. Here we show that in a rodent malaria parasite, *Plasmodium berghei*, conditional overexpression of AP2-G can be used to synchronously convert the great majority of the population into fertile gametocytes. This discovery allowed us to redefine the time frame of sexual commitment, identify a number of putative AP2-G targets and chart the sequence of transcriptional changes through gametocyte development, including the observation that gender-specific transcription occurred within 6 h of induction. These data provide entry points for further detailed characterization of the key process required for malaria transmission.

The ability to produce multiple specialized cell types based on one genotype is typically associated with multicellular organisms, but can be found in all branches of the tree of life. The causative agent of malaria, an apicomplexan parasite from the *Plasmodium* genus, is characterized by a complex life cycle involving a number of morphologically different stages adapted to different niches in its mammalian host or anopheline mosquito vector. These stages undergo linear transitions, with one notable exception: intracellular blood stages, which are associated with all symptoms of malaria, enter one of two developmental pathways. Following entry into a red blood cell (RBC), parasites either replicate asexually to form a schizont (which contains multiple merozoites able to invade new RBCs, leading to an increase in parasitaemia), or develop into sexual forms, male or female gametocytes, which are responsible for transmission to the mosquito vector[1]. The extent of gametocytogenesis varies in response to multiple environmental factors, implying a significant flexibility in fate determination at the level of the individual cell. The molecular mechanisms and stimuli regulating this process, however, remain poorly understood—although recently it has been shown that lysophosphatidylcholine (a human serum component) has a role in repressing gametocytogenesis[6].

In multiple model systems, differentiation into a particular cell type is triggered by key transcription factors acting as switches between different developmental pathways. Previously, AP2-G, a transcription factor from the apicomplexa-specific apiAP2 family, was shown to be necessary for gametocytogenesis in *Plasmodium* spp.[2,3], and its absence resulted in parasites unable to commit to sexual development (Fig. 1a). Here, we tested if overexpression of this factor could increase gametocyte production and enable the investigation of the uncharacterized earliest stages of gametocyte development.

To create a tightly controlled conditional overexpression system, two different gene expression modules were introduced into the genome of the rodent malaria parasite *Plasmodium berghei*. First, a constitutively expressed split Cre recombinase (diCre), able to catalyse recombination between *loxP* sequences when activated with rapamycin, was introduced into the *p230p* neutral locus of the parasite (Fig. 1b,c and Supplementary Fig. 1)[7]. The resulting parasite line provided efficient and rapid control over diCre activity, as shown by the ability to completely recombine a test plasmid both in vitro and in vivo, switching the expression from green to red fluorescent protein (Fig. 1d,e and Supplementary Fig. 2). The second module included modified *loxP* sites (*lox66* and *lox71*)[8] in a head-to-head orientation flanking a strong constitutive promoter (*hsp70*) used to express a selection marker (Fig. 1f). This module was inserted in front of the *ap2-g* open reading frame (ORF), interrupting and uncoupling its native promoter (Supplementary Fig. 3a). In this position, the unidirectional induced lox recombination event would invert the *hsp70* promoter and overexpress *ap2-g*.

Both modules were successfully inserted into a *P. berghei* reporter line containing a third module that expressed green and red fluorescent reporter markers in male and female gametocytes, respectively[9], generating PB_{GAMi}. PB_{GAMi} schizonts were synchronized in vitro and grown in vivo with ($PB_{GAMi}R^+$) or without ($PB_{GAMi}R^-$) rapamycin. Both populations were analysed at different time points using quantitative PCR (qPCR), light microscopy and flow cytometry (FACS). Recombination was detected in the $PB_{GAMi}R^+$ population immediately after induction and reached its maximum at ~12 h, eliminating the unedited locus (Fig. 1g and Supplementary Fig. 3b,c). In the $PB_{GAMi}R^-$ population, all parasites transformed

[1]Institute of Infection, Immunity and Inflammation, University of Glasgow, Glasgow, UK. [2]Department of Microbiology and molecular genetics, University of Vermont, Burlington, VT, USA. [3]Wellcome Trust Sanger Institute, Hinxton, Cambridge, UK. [4]Institute of Immunology and Infection Research, University of Edinburgh, Edinburgh, UK. [5]These authors contributed equally to this work: Robyn S. Kent, Katarzyna K. Modrzynska.
*e-mail: katarzyna.modrzynska@glasgow.ac.uk; ob4@Sanger.ac.uk; Andy.Waters@glasgow.ac.uk

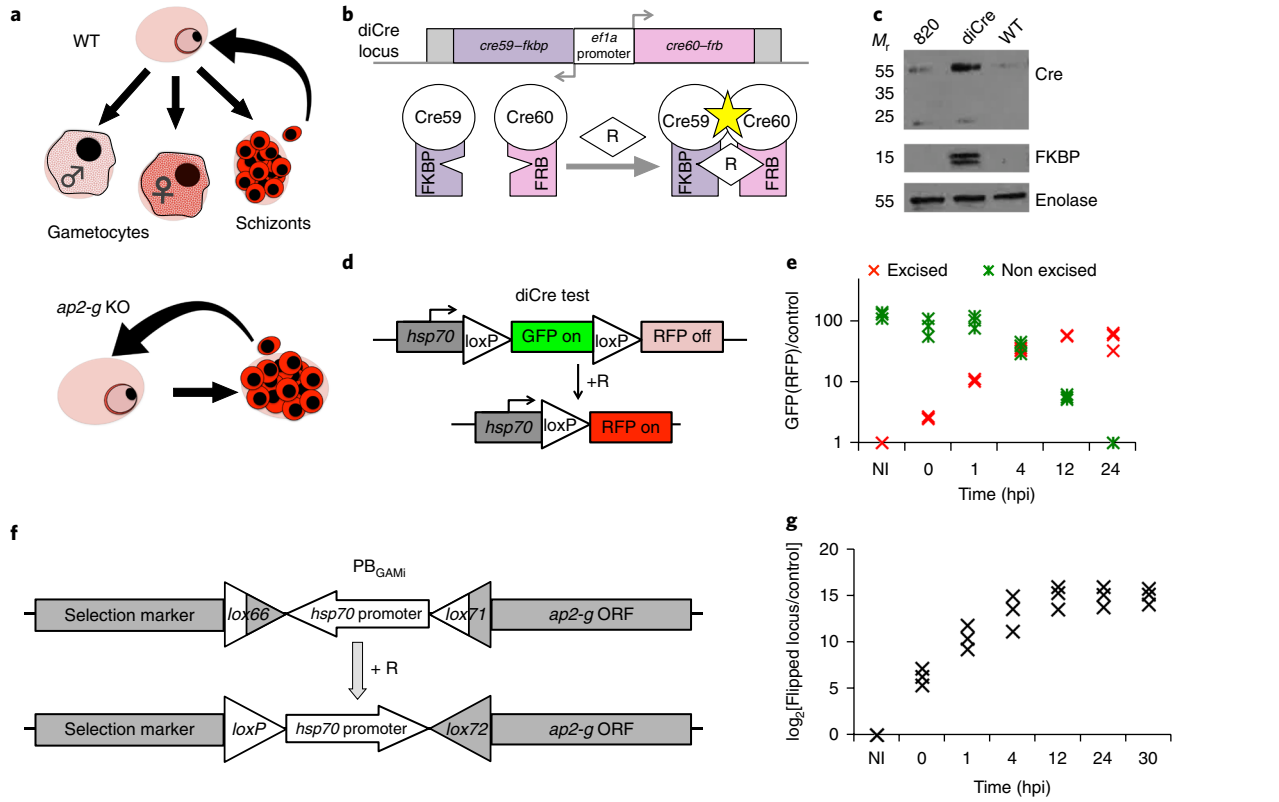

Fig. 1 | Establishment of an AP2-G-overexpression system. a, Top, a schematic diagram depicting the three developmental fates of a newly invaded ring-stage parasite. From the left, male gametocyte, female gametocyte and schizont (schizonts consist of daughter merozoites, which are capable of invading new RBCs and forming new rings). Bottom, parasites missing *ap2-g* undertake only asexual development. **b**, Top, the cassette inserted in the *P. berghei* 820 line expressing two Cre fragments fused to FKBP and FRB driven by the bidirectional *ef1a* promoter. Bottom, principle of reconstitution of Cre recombinase activity following addition of rapamycin (R). **c**, Western blot analysis showing expression of the two diCre system fragments in the cloned PB_{GAMi} line. The Cre antibody shows Cre60–FRB, and the FKBP antibody shows Cre59–FKBP. Three independent blots were completed with similar results. **d**, The design of the construct used to test diCre activity. **e**, qPCR quantification of edited and unedited test plasmid sequences in diCre test parasites at different time points after rapamycin induction. Three technical replicates of the samples generated within the same time course are shown. At each time point, DNA was harvested from an independently infected animal. NI, not induced. **f**, A schematic diagram of the *ap2-g* locus in PB_{GAMi} parasites before (top) and after (bottom) the editing event. **g**, qPCR quantification of the edited *ap2-g* locus in the PB_{GAMi} parasites. Three technical replicates of the samples generated within the same time course are shown. At each time point, DNA was harvested from an independently infected animal.

into asexual schizonts within 24 h, replicating the *ap2-g* knock-out (KO) phenotype and resulting in an increase of parasitaemia (Fig. 2a–d). In contrast, the $PB_{GAMi}R^+$ population did not produce schizonts (Fig. 2a) or increase in parasitaemia (Fig. 2d). Instead, many cells with gametocyte-like morphology appeared (Fig. 2a,b). Flow cytometry confirmed the expression of male and female reporter proteins in $PB_{GAMi}R^+$ from 12 h post induction (hpi; Fig. 2c and Supplementary Fig. 4). The combined percentage of male and female gametocytes in the population reached 70% in some experiments, and the total gametocyte proportion was always significantly higher ($P = 0.0021$, Student's unpaired *t*-test) than in WT (Fig. 2b). Importantly, GFP- and RFP-positive cells emerged following activation and formed male and female gametes, respectively, confirming that they are functional gametocytes (Fig. 2e). The relative ability of induced male gametocytes to replicate their genomes after activation was similar to WT, although their ability to go on to complete egress was reduced if compared to WT (Fig. 2e). This most likely reflects the fact that a reporter gene is necessarily an imperfect proxy for functional maturity. In our system, expression of the male marker from 12 h after induction (Supplementary Fig. 4) precedes functional maturity, and as a consequence, differences in the age distribution between synchronous induced and asynchronous WT-marker-positive male gametocytes must result in differences in apparent functional maturity.

Experimental evidence from *P. falciparum* has suggested that commitment to gametocytogenesis occurs in the blood stage cycle before the appearance of gametocytes, resulting in the production of a committed schizont/merozoite population destined to develop into gametocytes following erythrocyte invasion[10]. To determine the period during which *P. berghei* asexual parasites are sensitive to reprogramming, we induced *ap2-g* overexpression at multiple time points during the 24 h cycle of asexual development (at 2, 4, 8, 12, 18, 22 h after merozoite invasion). Parasites induced before 12 hpi could be transformed with decreasing efficiency into gametocytes within the same developmental cycle (Fig. 2f and Supplementary Fig. 5a). In marked contrast, parasites induced after 12 hpi all developed into asexual schizonts, and gametocyte conversion was observed only following invasion in the next cycle. The timing of induction did not appear to have a marked effect on the cumulative number of gametocytes formed (Supplementary Fig. 5a,b). The male-to-female ratio in induced gametocytes was within the range observed in the parental population (Fig. 2b), and any apparent shifts in sex ratio with time of induction (Fig. 2f) may simply reflect the earlier upregulation of the male marker, as discussed above.

The inducible and synchronized sexual commitment provided an opportunity to assess transcriptional changes in developing gametocytes. Synchronous schizonts (22 hpi) were induced in vivo with rapamycin to obtain a single wave of commitment after reinvasion,

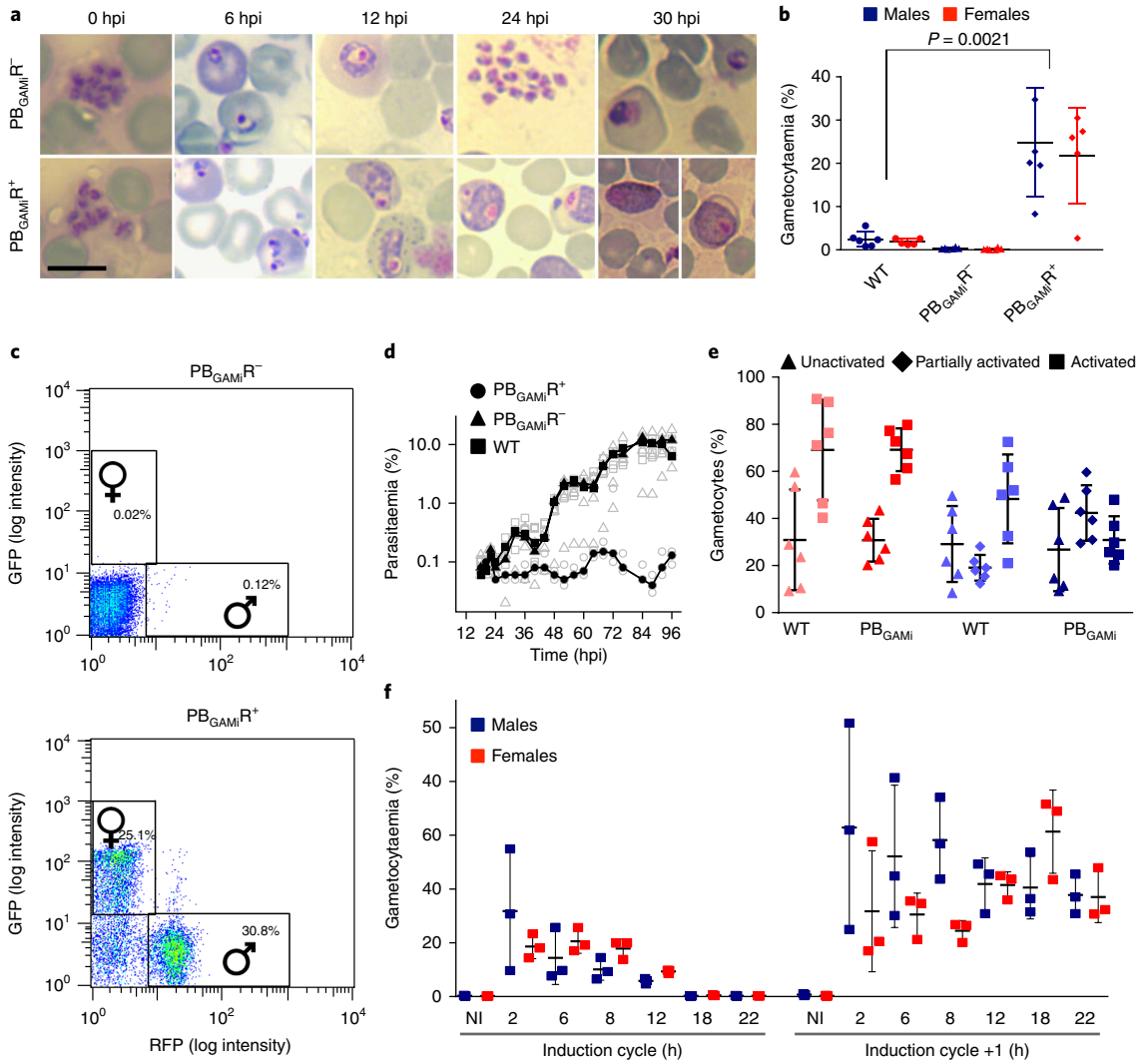

Fig. 2 | AP2-G overexpression results in gametocyte conversion. a, Parasite morphology in Giemsa-stained thin blood smears in PB$_{GAMi}$R$^-$ (top) and PB$_{GAMi}$R$^+$ (bottom) populations, demonstrating evident production of gametocytes in the induced parasites. Representative pictures from 3 independent biological replicates for each time point are shown. Scale bar, 10 µm. **b**, Gametocyte conversion rates in PB$_{GAMi}$R$^-$ and PB$_{GAMi}$R$^+$ parasites compared to the parental line. Gametocytaemia shown as percentage of infected cells expressing male (blue) or female (red) markers in FACS analysis 30 h post induction. Means, standard deviations and individual data points from 5 independent biological replicates are shown. Statistical significance in total gametocyte numbers determined with a two-tailed, unpaired Student's *t*-test. **c**, FACS profiles of PB$_{GAMi}$R$^-$ and PB$_{GAMi}$R$^+$ parasites 30 h after induction, representative for 5 biologically independent experiments. The gating strategy for male and female parasite populations is shown. **d**, Parasitaemia in PB$_{GAMi}$R$^-$/R$^+$ population compared to WT parasites defined as percentage of DNA-positive RBCs in FACS analysis. Median and individual measurements from 3 independent biological replicates are shown. **e**, Percentage of unactivated, activated and partially activated cells in WT and PB$_{GAMi}$R$^+$ gametocytes. Full activation is defined as successful production of male gametes and their emergence out of the blood cells (exflagellation). Partial activation of male gametocytes is identified when DNA replication has occurred (increase in Hoechst 33342 intensity) but exflagellation from the RBC has not occurred. Means, standard deviations and individual data points from 5 independent biological replicates are shown. Statistical significance assessed using unpaired two-tailed Student's *t*-test. **f**, Gametocyte conversion rates in PB$_{GAMi}$ parasites induced in vivo at the different time points post invasion. Total proportion of gametocytes generated within the same cycle (maximum measurement until 40 hpi) and after subsequent reinvasion (64 hpi) is shown for the same infection. NI, not induced. Means, standard deviations and individual data points from 3 independent biological replicates are shown.

and RNA sequencing (RNA-seq) libraries were prepared from PB$_{GAMi}$R$^-$ and PB$_{GAMi}$R$^+$ parasites harvested at 6 h intervals between 0 and 30 h post induction. Initially, data were used to examine the level of expression of functional *ap2-g* transcript, which was absent in the PB$_{GAMi}$R$^-$ population but detected in the PB$_{GAMi}$R$^+$ population, reaching its maximum at 12 h and exceeding native expression within the population[11] within the first 6 h (Fig. 3a and Supplementary Fig. 6). Analysis of the remainder of the transcriptome confirmed that at 30 hpi the PB$_{GAMi}$R$^-$ population was similar to the transcriptome of asexual schizonts, whereas PB$_{GAMi}$R$^+$ was indistinguishable from purified gametocytes, indicating that the cells that did not develop into gametocytes either produced the gametocyte transcriptome or were transcriptionally silent (Fig. 3b). The PB$_{GAMi}$R$^{+/-}$ populations diverged gradually from 6 h (58 genes) to 30 h, when 2,676 genes showed some level of differential regulation (Fig. 3c and Supplementary Table 2). The dynamics of gene expression in PB$_{GAMi}$R$^+$ parasites closely mirrored the expected patterns of developing WT gametocytes, as indicated by gene ontology (GO) terms associated with different time points (Fig. 3c and Supplementary Table 3), which shifted from protein kinases and

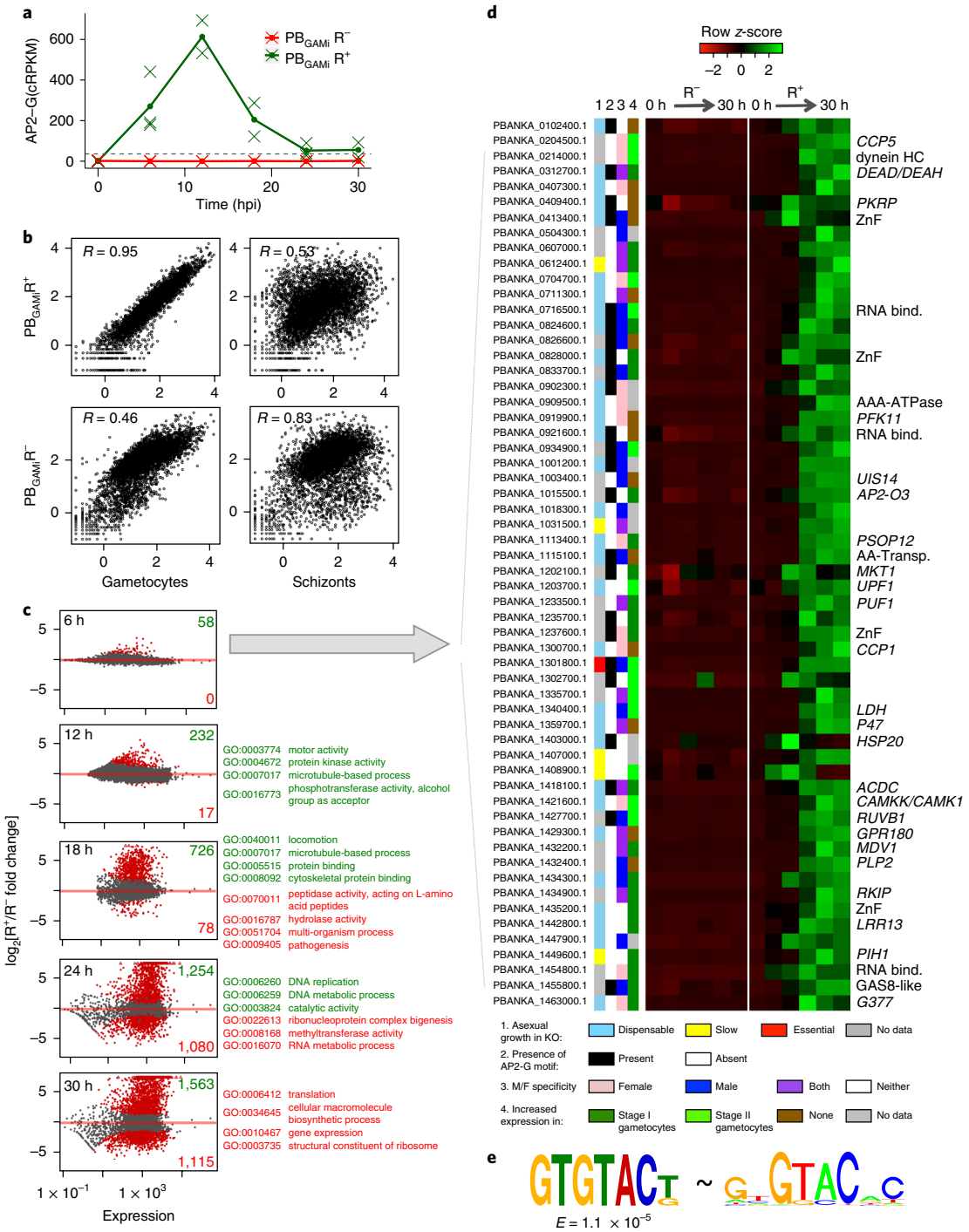

Fig. 3 | Transcriptome changes in PB$_{GAMi}$R$^-$ and PB$_{GAMi}$R$^+$ parasites reveal a gametocyte-specific transcriptional programme. a, Expression of the *ap2-g* transcript in PB$_{GAMi}$R$^-$ and PB$_{GAMi}$R$^+$ populations. Corrected reads per kilobase per million reads (cRPKM) calculated as seen in Supplementary Fig. 6. Means and individual data points from 3 (0, 6 and 24 h) or 2 (12, 18 and 30 h) independent biological replicates are shown. Horizontal black dashed line indicates maximal native *ap2-g* RNA expression in the WT population[11]. **b**, Comparison of transcriptomes (RPKMs) from PB$_{GAMi}$R$^-$ and PB$_{GAMi}$R$^+$ populations 30 hpi to purified gametocytes and schizonts transcriptomes. *R*, Spearman's rank correlation coefficient. Correlation values representative for $n = 3$ experiments. **c**, Differential expression analysis between PB$_{GAMi}$R$^-$ and PB$_{GAMi}$R$^+$ populations at different time points. Plots show log$_2$ fold change of gene expression versus expression levels, with differentially expressed genes marked in red. Numbers of genes overexpressed in PB$_{GAMi}$R$^-$ (red) and PB$_{GAMi}$R$^+$ (green), and example GO terms enriched within each group, are shown next to each graph. All samples for transcriptome analysis were generated from three independent time course experiments. **d**, Genes responding early to AP2-G overexpression. Shown are: knockout growth phenotype in asexual blood stages[14], sex specificity of expression in *P. berghei*[15], gametocyte specificity in *P. falciparum*[28], presence of AP2-G motif(s) within 2 kb upstream of the start codon, and gene expression profile through the time course. Available gene aliases or functional description according to the PlasmoDB database are shown on the right of the expression profile. AA-Transp., amino acid transporter; AAA-ATPase, AAA-family ATPase; dynein HC, dynein heavy chain; GAS8-like, GAS8-like protein; RNA bind., RNA binding protein; ZnF, zink-finger protein. **e**, The DNA motif enriched upstream of genes in **d** (left) compared with the known AP2-G binding motif[2,16] (right).

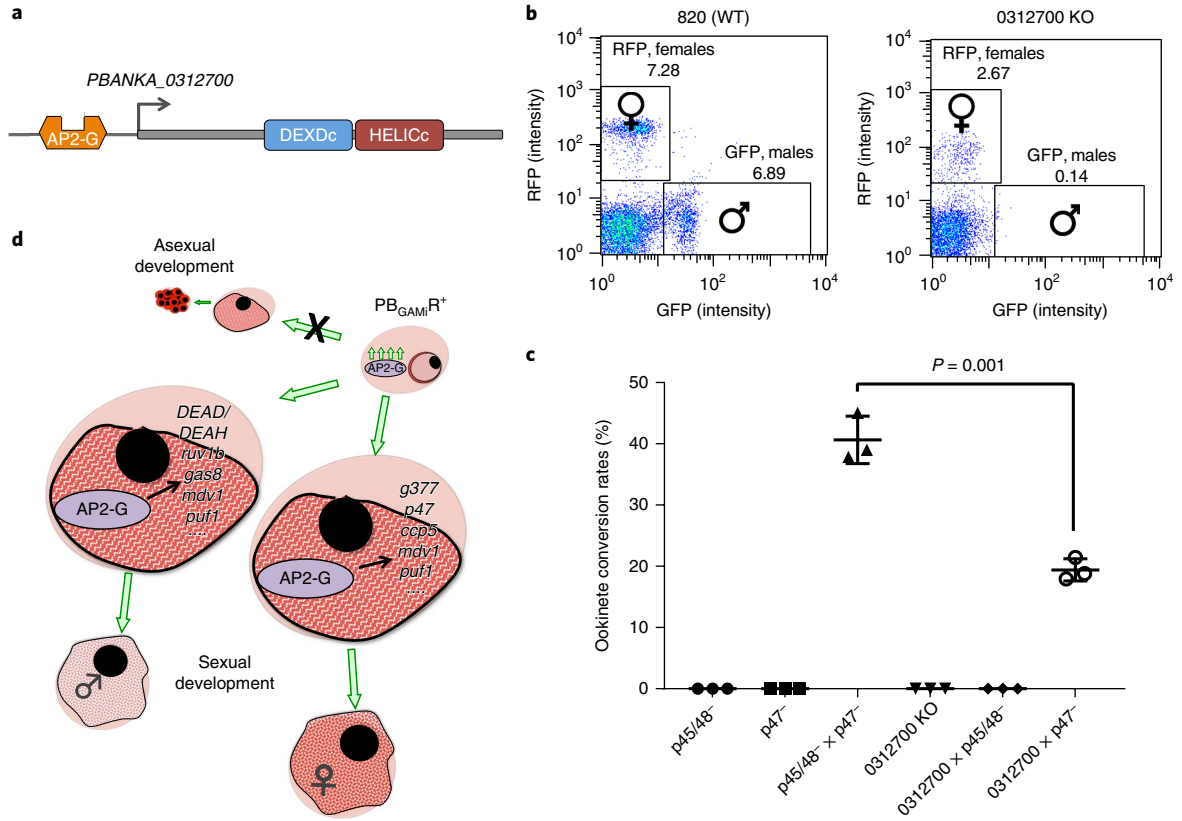

Fig. 4 | *PBANKA_0312700* is an AP2-G-induced gene involved in gametocyte development. a, The *PBANKA_0312700* gene structure with conserved helicase domains. The putative AP2-G binding motif is marked. **b**, Representative FACS analysis (from 4 independent experiments) showing loss of male gametocytes in the *PBANKA_0312700* KO. **c**, Ookinete conversion in *PBANKA_0312700* KO crossed with lines producing only viable females (*p48/45*$^{-}$) or males (*p47*$^{-}$), showing that the defective gametocyte development is male-specific. Means, standard deviations and individual data points from three independent biological replicates are shown. Statistical significance was determined with a two-tailed, unpaired Student's *t*-test. **d**, Model of AP2-G function in gametocyte commitment.

motor proteins of the male gametocyte at 12 h, to cytoskeleton organization (18 h) and the DNA replication machinery (24 h). As expected, translationally repressed transcripts that are known to be stored by the mature female gametocyte[12] were induced at later time points (Supplementary Fig. 7).

Of particular interest were the 58 genes responding already at the 6 h time point, which included conserved early gametocyte markers such as *mdv1*[13] as well as proteins potentially involved in nucleic acid binding, including four zinc finger proteins, three RNA binding proteins, two helicases and one other apiAP2 transcription factor (Fig. 3d). In comparison with the rest of the genome, this subset was significantly enriched ($P = 1.387 \times 10^{-5}$, Fisher exact tests) in genes dispensable for asexual blood stages[14], and many of its members are known to be specific to the male or female sex in mature gametocytes[15]. The promoter regions of these genes were also significantly ($E = 1.1 \times 10^{-5}$) enriched in a GTGTAC(T/G) motif resembling closely the known DNA-binding motif for the AP2 domain of AP2-G (Fig. 4e)[16], suggesting that at least some of them may be direct downstream targets of AP2-G. Comparison with the available datasets from human malaria *Plasmodium falciparum* revealed that almost all of these genes (35 out of the 49 with identified syntenic orthologues) are upregulated in the early phase of gametocytogenesis (days 1 and 3), suggesting that the function of these genes is shared between different *Plasmodium* species (Fig. 3d and Supplementary Fig. 8). In contrast, the genes that are upregulated and co-expressed with *ap2-g* in *P. falciparum*[3,17] predominantly encode secreted proteins that are not present in the *P. berghei* genome, and are thought to be associated with the extensive remodelling of the erythrocyte that is uniquely undertaken by *P. falciparum* gametocytes[18].

To confirm a role of one of these conserved, induced genes in gametocytogenesis, we disrupted the predicted DEAD/DEAH helicase, *PBANKA_0312700* (Fig. 4a and Supplementary Fig. 9), which has a putative AP2-G binding site 650 bp upstream of its start codon and shows a robust transcriptional response at 6 hpi and is expressed in both male and female gametocytes. The mutant completely lacked mature male gametocytes, as tested by FACS (Fig. 4b) and blood smears. Female gametocytes were, however, viable and able to transmit when crossed with a strain producing viable males (Fig. 4c). These findings were consistent with a predominant function for PBANKA_0312700 in male gametocyte development, although the reduction in ookinete conversion when compared to a fully viable female-only strain (Fig. 4c) could also indicate a downstream role for this helicase in female gametocyte development or fertilization.

Here we have shown that inducible expression of AP2-G is sufficient to induce synchronous gametocytogenesis in a *Plasmodium* parasite, overriding the default asexual replication programme and leading to the generation of functional gametocytes. Importantly, this conversion could be initiated within the same developmental cycle, proving that the fate of the young intraerythrocytic parasites is not irreversibly determined. This finding is seemingly at odds with previous studies with human parasites where the existence of sexually pre-committed schizonts producing next-generation gametocytes has been reported[4,10,17]. Our data may simply reflect significant differences in life cycle regulation between the two *Plasmodium*

parasites—gametocytogenesis in *P. falciparum* uniquely takes ~12 d, which is significantly longer than other *Plasmodium* spp., and *P. falciparum* gametocytes also possess a distinctive morphology. Alternatively, our discovery suggests a more general plasticity in commitment and an extended time window during which environmental factors[6] and epigenetic pre-programming[4,5] can impact the number of gametocytes. In that scenario, a proportion of the schizonts would be predisposed to generate gametocytes, but the final, irreversible commitment would be a late event in asexual blood stage development in the next cycle depending solely on AP2-G acting as a switch between the two transcriptional fates of the cell. According to that theory, *P. falciparum* parasites could be converted within the same cycle, but assays that would capture this possibility have not yet been developed or tested. Instead, our ability to bypass any upstream events allowed us to reveal the early transcriptional programme downstream of AP2-G, which appears to be shared between the two parasites. Intriguingly, many of these early response genes have a strongly sex-specific expression profile[15] or KO phenotype (including *PBANKA_0312700* tested here), suggesting that AP2-G may regulate different subsets of genes in both male and female precursors (Fig. 4d). This raises the possibility that commitment to the male or female sex either precedes or is simultaneous with AP2-G-mediated gametocytogenesis. This hypothesis has also been proposed in recent work capturing early transcription events in *P. falciparum*[19], where certain genes with sex-specific phenotypes were shown to be regulated independently of AP2-G.

In summary, the AP2-G overexpression system allowed full control of *Plasmodium* gametocytogenesis, and generated findings related to sexual commitment for future investigation. Equally, the application of the concept of the conditional inducible commitment may be extended to other apicomplexan parasites in which sexual development is less tractable, leading to useful insights regarding the transmission in these species.

Methods

Rodent malaria parasites and their maintenance. All experiments were performed using the *Plasmodium berghei* 2.34 ANKA strain and its modifications maintained in female, outbred mice (Theiler's original (TO)) 8–12 weeks of age. The infections were initiated by intraperitoneal or intravenous injection of either the frozen parasite stock or blood from an infected donor mouse, and monitored daily using Giemsa-stained thin blood smears. All animal procedures were conducted under project licenses issued by the UK Home Office and with local ethical approval of the Animal Welfare and Ethical Review Body of the Wellcome Trust Sanger Institute and the University of Glasgow Ethics Committee. For qualitative experiments (genotyping and western blots), one mouse per strain was used in each of the experiments. For quantitative experiments, the numbers were adjusted based on the variability of the studied trait and the effect size of interest, and are included in the description of experimental results. All animals/samples were assigned a number, and the data were initially analysed without the knowledge of the infection type or conditions/treatment to ensure minimal bias.

Generation of the mutant parasite lines. The non-fluorescent strain c115cy1 HP and its derivate 820, expressing GFP and RFP markers in male and female gametocytes, respectively[9], were used to create diCre-expressing lines. The marker-free HP diCre and 820 diCre lines were generated using the GIMO (gene-in marker out) approach described previously[20] and presented in Supplementary Fig. 1. Briefly, a positive–negative selection marker was inserted into the parasite's neutral *p230p* locus via homologous recombination. After positive selection and cloning by serial dilution, the second transfection followed by negative selection was used to replace the marker with the diCre expression cassette, and a second cloning step was performed. The diCre test line was generated by transfecting HP diCre with a centromeric, single-copy plasmid containing a *hsp70* promoter, a floxed GFP and RFP separated by a loxP site, as shown in Fig. 1g. The 820 diCre line was transfected with linear DNA modifying the *ap2-g* locus (Supplementary Fig. 3) to generate PB_{GAMi}. A *PBANKA_0312700* KO line was generated in 820 parasites by replacing the gene with a positive–negative selection marker, as shown in Supplementary Fig. 8.

All transfections were performed using an established *P. berghei* schizont electroporation protocol. Parasites were grown to 1–6% parasitaemia in mice treated with 1.2 mg of phenylhydrazine (Sigma) 2 d before the infection, and collected by cardiac puncture before transfer to schizont media (RPMI 1640 + L-glutamine + 25 mM HEPES, supplemented with 25% foetal bovine serum, 10 mM sodium bicarbonate and penicillin–streptomycin). After overnight culture at 37 °C in an atmosphere of 5% CO_2, 5% O_2 and 90% N_2, schizonts were isolated by 15 min of centrifugation at 500*g* on a cushion of 55% Nycodenz (Lucron Bioproducts). The schizonts were harvested from the interface and then electroporated with 1–10 µg of linear DNA or plasmid using an Amaxa Nucleofector device and Basic Parasite Nucleofector Kit 2 according to the manufacturer's instructions. Parasites were intravenously injected into new mice and recovered for 25 h before selection with pyrimethamine (7 µg ml^{-1} in drinking water) or 5-fluorocytosine (1.5 mg ml^{-1} in the drinking water, HP diCre and 820 diCre lines only). Selected parasites were recovered ~7 d post transfection. All lines were cloned by limiting dilution before the next modification step.

Genome editing in diCre parasites. *P. berghei* parasites were synchronized by overnight culture in schizont media and a Nycodenz gradient was used to harvest schizonts, as described above. Purified schizonts were intravenously injected into naive mice, where they maintained their synchronicity for 48 h. Rapamycin (Sigma) was dissolved in DMSO to 4 mg ml^{-1} to generate the stock solution. DiCre test parasites were induced either in vitro and in vivo. For in vitro induction, parasites were removed from the host by cardiac puncture 2 h post invasion (hpi) and cultured in schizont media with 200 mM rapamycin. For in vivo induction, the host animals were injected intraperitoneally with 4 mg kg^{-1} rapamycin 2 hpi. Parasites were harvested at various time points via tail bleed or cardiac puncture for DNA and flow cytometry analysis. To generate a population of invading merozoites overexpressing AP2-G, the PB_{GAMi} line was induced 22 hpi by 4 mg kg^{-1} of rapamycin injection and its development was analysed in the next invasion cycle, unless specified otherwise. In each case, an uninduced control population of parasites was analysed in parallel.

DNA extraction for PCR or qPCR genotyping. To extract parasites from host blood, ~1 ml of heparinized whole blood was collected by cardiac puncture. Leukocyte depletion was achieved by filtration through two sequential Plasmodipur filters (Europroxima) according to the manufacturer's instructions. Remaining cells were resuspended in 10 volumes of pre-chilled erythrocyte lysis buffer (150 mM NH_4Cl; 10 mM $KHCO_3$; 1 mM EDTA) and incubated on ice for 15 min. After lysis, parasites were pelleted by centrifugation for 8 min at 450*g* and washed with 1x phosphate buffered saline until complete removal of the colouration of supernatant, and either stored at −20 °C for later DNA isolation or processed immediately.

In the second part of the protocol, the fresh or frozen parasite pellet was resuspended in 700 µl TNE buffer (50 mm Tris–HCl, pH 7.4, 100 mm NaCl, 0.1 mm EDTA), supplemented with 200 µg RNase and 1% SDS. This mixture was incubated for 10–15 min at 37 °C, after which 200 µg proteinase K was added and the solution incubated for a further 1 h. Then a standard phenol and chloroform extraction protocol followed by ethanol precipitation[21] was used to extract the DNA from the lysate. Quality and concentration of the nucleic acids were measured using a UV-Vis spectrophotometer (NanoDrop, Thermo Scientific).

PCR genotyping. Genotyping strategies for genetically modified parasites are presented in Supplementary Figs. 1–3 and 9, and the primer sequences are given in Supplementary Table 1. All PCR reactions were performed using *Taq* DNA Polymerase (NEB) and the following PCR programme: 94 °C 30 s, (94 °C 30 s, Tm °C 30 s, 72 °C 1 min) x 30, 72 °C 10 s, 4 °C, where Tm °C was a annealing temperature specific for each primer pair. PCR products were resolved on a 1% agarose gel supplemented with 1:10,000 SYBR Safe reagent and visualized using Gel Doc XR + Gel Documentation System.

qPCR genotyping. qPCR primers were designed as shown in Supplementary Figs. 2 and 3 and full primer sequences are shown in Supplementary Table 1. The amplification reaction was set up using 50 ng of DNA and QuantiTect Sybr Green PCR Kit (Qiagen) according to the manufacturer's instructions. The reaction was incubated in StepOne Real-Time PCR System (Applied Biosystems) using the following programme: 95 °C 10 min, (95 °C 15 s, 60 °C 1 min) × 40, 95 °C 15 s, 60 °C 1 min, gradient +0.3 °C, 95 °C 15 s.

At least three technical replicates of each measurement were taken. A neutral sequence present in both induced and uninduced sample was amplified as a reference and DNA from uninduced population was used as control. The fold change calculations were based on the ΔΔCt method (http://www3.appliedbiosystems.com/cms/groups/mcb_support/documents/generaldocuments/cms_042380.pdf).

Western blot analysis of diCre production. Protein pellets (isolated as described for the DNA extraction) were suspended in 5× pellet volume of RIPA lysis buffer (50 mM Tris–HCl, pH 8.0, 150 mM NaCl, 1 mM EDTA, 0.5% sodium deoxycholate, 0.1% SDS, 1 % triton X-100) and incubated on ice for ~30 min. The lysate was spun for 10 min at 4 °C, at 16,000*g* and the supernatant was combined with 4× SDS gel-loading buffer (62.5 mM Tris-H_3PO_4, pH 7.5, 1 mM EDTA, 2% SDS, 10 mM DTT, 1 mM NaN_3 and 33% glycerol) and fresh 15% β-mercaptoethanol. Samples were boiled at 100 °C for 5 min and loaded on SDS-PAGE gradient gel (Biorad). Electrophoresis was performed using Mini-PROTEAN Tetra cell electrophoresis

chamber (Qiagen) for 2 h at 120 V. The resolved proteins were transferred on Whatman nitrocellulose membrane using a trans-blot electrophoretic transfer system according to the manufacturer's protocol, blocked with 5% milk PBST and probed with the antibodies against FKBP-12 (1:500), Cre (1:500) and enolase (1:1,000) (all Abcam), followed by a compatible HRP-labelled secondary antibody. Enhanced chemiluminescence system (ECL) was used to visualize the proteins on X-ray film.

Flow cytometry analysis diCre activity and gametocyte production. RBCs for analysis were collected from tail drops, cardiac puncture or parasite cultures. Cells were suspended in pre-warmed rich PBS with Hoechst 33342 dye and stained for 30 min at 37 °C. Stained samples were washed and resuspended in flow cytometry buffer (10% rich PBS, 1 mM EDTA in PBS) and analysed using LSR-II flow cytometer (Becton Dickinson) with the following emission/excitation settings: Hoechst (DAPI, yellow laser, 350 nm) 450/50, GFP (FITC 488 nm) 488/10 and RFP (PE 561 nm) 585/15. At least 500,000 events were acquired for each sample. Initial gating was performed using forward and side scatter to exclude the events below the size and granularity thresholds of RBCs. Then FCS-H FCS-W gating served to isolate single RBCs and followed by Hoechst staining selecting parasite-infected cells as shown in Supplementary Fig. 4a. For the 820 line and its derivatives, GFP and RFP gates were used to select the male and female gametocytes respectively. For the diCre -test line the GFP, RFP and bifluorescent populations were selected to show different stages of excision as shown in Supplementary Fig. 2d. In each experiment involving 820 modifications uninfected blood and WT 820 line were used as controls. In fluorescence switching experiments, both non-fluorescent parasites and lines constitutively expressing GFP or RFP only (with appropriate strength promoters) were used as controls (Supplementary Fig. 2e).

Exflagellation/emergence. Tail drops of blood were collected in 500 µl 37 °C schizont media (as above, unactivated) or 21 °C ookinete media (RPMI 1640, 10% FCS, xanthurenic acid, activated) and incubated at the appropriate temperature for 30 min. Ter119 PEcy7 (https://www.thermofisher.com/antibody/product/TER-119-Antibody-clone-TER-119-Monoclonal/25-5921-82) and Hoechst were added to a final concentration of 1:200 and a total volume of 700 µl and intensively vortexed. Samples were incubated at their appropriate temperature for an additional 20 min, vortexing every 5 min. Stained samples were washed in 500 µl rPBS and resuspended in 500 µl FACS buffer for analysis. Male and female gametocytes were identified by their GFP and RFP signal respectively using the gating presented in Supplementary Fig. 4a. Gametocytes were considered unactivated if positive for PEcy7 Ter119 staining and activated if this staining is negative. Only gametocytes were included in quantification of activation.

Time course of variable gametocyte induction and flow cytometry quantification. Mice were injected with synchronized PB_{GAMi} parasites and induced *in vivo* with rapamycin at multiple time points post invasion (2, 6, 8, 12, 18 and 22 h) as described previously. Samples were obtained from tail drops and the parasitaemia (Hoechst 33342-positive cells) and percentage of male (GFP) and female (RFP) gametocytes were quantified every 4 h from 8 h post invasion using flow cytometry. Since sex-specific fluorescence makers became detectable only from 16 h post invasion (Supplementary Figure 4B), any gametocytes originating from the second cycle after induction would become detectable only after 40 hpi post invasion (24 h cycle + 16 h maturation). We therefore considered the highest measurement taken before 40 hpi as the number of gametocytes produced within the first cycle. The last measurement taken at 64 hpi was considered as the total number of gametocytes produced within both cycles.

Time course of gametocyte induction, RNA extraction and RNA-seq library preparation. Mice were injected with synchronized PB_{GAMi} parasites and induced with rapamycin at 22 h as described previously. Parasites were harvested at different time points post induction via cardiac puncture, filtered, extracted from RBC and washed in 1× PBS as for DNA isolation. Parasite pallets were resuspended in 1 ml of Trizol reagent (Ambion) lysed for 10 min at room temperature and stored at −80 °C for later RNA extraction.

Complete RNA was isolated from the samples using Trizol/chloroform extraction followed by isopropanol precipitation[21] and its concentration and integrity was verified using Agilent Bioanalyzer (RNA 6000 Nano kit) and NanoDrop 1000 spectrophotometer. 1–2 µg of total RNA from each sample (or complete sample if the yield was lower) was used for mRNA isolation (Magnetic mRNA Isolation Kit, NEB). First strand cDNA synthesis was performed using the SuperScript III First-Strand Synthesis System and a 1:1 mix of oligo(dT) and random primers (Invitrogen). The DNA-RNA hybrids were purified using Agencourt RNACleanXP beads (Beckman Coulter) and the second cDNA strand was synthetized using a 10 mM dUTP nucleotide mix, DNA Polymerase I (Invitrogen) and RNAseH (NEB) for 2.5 h at 16 °C. The long cDNA fragments were purified and fragmented using a Covaris S220 system (duty cycles, 20; intensity, 5; cycles per burst, 200; time, 30 s). The ~200-bp-long fragments were end-repaired, dA-tailed and ligated to 'PCR-free' adapters[22] with index tags using NEBNext modules according to the manufacturer's instructions. Excess adapters were removed by two rounds of clean-up with 1 volume of Agencourt AMPure XP beads. Final libraries were eluted in 30 µl water, quality-controlled using Agilent Bioanalyzer (High Sensitivity DNA chip) digested with USER enzyme (NEB) and quantified by qPCR. For some libraries, an additional 5 cycles of PCR amplification were performed, using KAPA HiFi HotStart PCR mix and Illumina tag-specific primers to obtain enough material for sequencing. Pools of indexed libraries were sequenced using an Illumina HiSeq2500 system (100 bp paired-end reads) according to manufacturer's manual. All samples were generated in duplicates or triplicates and uninduced controls were always generated and processed in parallel. Raw data are available through GEO database repository (GSE110201).

RNA-seq data analysis. The generation of raw data in the form of 'cram' files quality control and adapter trimming was performed using the default analysis pipelines of the Sanger Institute. The raw data were transformed into paired 'fastq' files using Samtools software (ver. 1.3.1). The generated reads were re-aligned to *Plasmodium berghei* genome (PlasmoDB-30 release) in a splice aware manner with HISAT2[23] using the '–known-splicesite-infile' option within the splicing sites file generated based on the current genome annotation. Resulting 'bam' files were sorted and indexed using Samtools and inspected visually using the Integrated Genome Viewer (ver. 2.3.91). A HT-seq python library[24] was used to generate reads counts for all genes for further processing. Differential expression calculation and correlation analysis was performed and visualized using R studio software (v. 1.0.136) with the DESeq2, ggplot2 and GMD packages[25].

The reference schizont and gametocytes transcriptome datasets were downloaded from[26] and compared to the generated samples using Spearman's rank correlation coefficient. The enrichment for the translationally repressed genes in different differentially expressed datasets was performed using Fisher exact test. For the analysis of male and female specificity and growth rates, the data from refs [15,14] respectively was used. Growth rate above 0.8 was considered normal, between 0.8 and 0.2 it was decreased, and below 0.2 the gene was considered essential. The gene was considered male/female specific if its expression in the gametocytes of the given sex was at least 10-fold greater than in the opposite sex as well as in the asexual parasites. DOZI translationally repressed genes were defined as the ones enriched in both DOZI and CITH RIP-ChIP datasets[27]. Comparison with *P. falciparum* data was performed using the available PF datasets[3,28] and synteny information[11]. Genes were considered as overexpressed in early gametocytes stages if their expression was at least 2-fold greater than in the matched asexual population[28].

De novo regulatory motif discovery was performed using DREME software[29] and sequences 2 kb upstream of the translation sites of the genes upregulated 6 h post rapamycin induction as the input set and the promoters of the remaining genes in the genome as the reference set.

Reporting Summary. Further information on research design is available in the Nature Research Reporting Summary linked to this article.

Data availibility. RNA-seq data generated in this study are available through the GEO database repository (accession number GSE110201).

Received: 19 November 2017; Accepted: 24 July 2018;
Published online: 3 September 2018

References

1. Meibalan, E. & Marti, M. Biology of malaria transmission. *Cold Spring Harb. Perspect. Med.* **7**, a025452 (2017).
2. Sinha, A. et al. A cascade of DNA-binding proteins for sexual commitment and development in *Plasmodium*. *Nature* **507**, 253–257 (2014).
3. Kafsack, B. F. C. et al. A transcriptional switch underlies commitment to sexual development in malaria parasites. *Nature* **507**, 248–252 (2014).
4. Brancucci, N. M. B. et al. Heterochromatin protein 1 secures survival and transmission of malaria parasites. *Cell Host Microbe* **16**, 165–176 (2014).
5. Filarsky, M. et al. GDV1 induces sexual commitment of malaria parasites by antagonizing HP1-dependent gene silencing. *Science* **359**, 1259–1263 (2018).
6. Brancucci, N. M. B. et al. Lysophosphatidylcholine regulates sexual stage differentiation in the human malaria parasite *Plasmodium falciparum*. *Cell* **171**, 1532–1544 (2017).
7. Jullien, N., Sampieri, F., Enjalbert, A. & Herman, J.-P. Regulation of Cre recombinase by ligand-induced complementation of inactive fragments. *Nucleic Acids Res.* **31**, e131 (2003).
8. Albert, H., Dale, E. C., Lee, E. & Ow, D. W. Site-specific integration of DNA into wild-type and mutant lox sites placed in the plant genome. *Plant J.* **7**, 649–659 (1995).
9. Mair, G. R. et al. Universal features of post-transcriptional gene regulation are critical for *Plasmodium* zygote development. *PLoS Pathog.* **6**, e1000767 (2010).
10. Bruce, M. C., Alano, P., Duthie, S. & Carter, R. Commitment of the malaria parasite *Plasmodium falciparum* to sexual and asexual development. *Parasitology* **100**, 191–200 (1990).
11. Otto, T. D. et al. A comprehensive evaluation of rodent malaria parasite genomes and gene expression. *BMC Biol.* **12**, 86 (2014).

12. Mair, G. R. et al. Regulation of sexual development of *Plasmodium* by translational repression. *Science* **313**, 667–669 (2006).
13. Lal, K. et al. Plasmodium male development gene-1 (mdv-1) is important for female sexual development and identifies a polarised plasma membrane during zygote development. *Int. J. Parasitol.* **39**, 755–761 (2009).
14. Bushell, E. et al. Functional profiling of a *Plasmodium* genome reveals an abundance of essential genes. *Cell* **170**, 260–272 (2017).
15. Yeoh, L. M., Goodman, C. D., Mollard, V., McFadden, G. I. & Ralph, S. A. Comparative transcriptomics of female and male gametocytes in *Plasmodium berghei* and the evolution of sex in alveolates. *Genomics* **18**, 734 (2017).
16. Campbell, T. L., De Silva, E. K., Olszewski, K. L., Elemento, O. & Llinás, M. Identification and genome-wide prediction of DNA binding specificities for the ApiAP2 family of regulators from the malaria parasite. *PLoS Pathog.* **6**, e1001165 (2010).
17. Poran, A. et al. Single-cell RNA sequencing reveals a signature of sexual commitment in malaria parasites. *Nature* **551**, 95–99 (2017).
18. Tibúrcio, M., Sauerwein, R., Lavazec, C. & Alano, P. Erythrocyte remodeling by *Plasmodium falciparum* gametocytes in the human host interplay. *Trends Parasitol.* **31**, 270–278 (2015).
19. Painter, H. J., Carrasquilla, M. & Llinás, M. Capturing in vivo RNA transcriptional dynamics from the malaria parasite *Plasmodium falciparum*. *Genome Res.* **27**, 1074–1086 (2017).
20. Lin, J. et al. A novel 'gene insertion/marker out' (GIMO) method for transgene expression and gene complementation in rodent malaria parasites. *PLoS ONE* **6**, e29289 (2011).
21. Chomczynski, P. A reagent for the single-step simultaneous isolation of RNA, DNA and proteins from cell and tissue samples. *Biotechniques* **15**, 532-4–536-7 (1993).
22. Kozarewa, I. et al. Amplification-free Illumina sequencing-library preparation facilitates improved mapping and assembly of (G+C)-biased genomes. *Nat. Methods* **6**, 291–295 (2009).
23. Kim, D., Langmead, B. & Salzberg, S. L. HISAT: a fast spliced aligner with low memory requirements. *Nat. Methods* **12**, 357–360 (2015).
24. Anders, S., Pyl, P. T. & Huber, W. HTSeq–a Python framework to work with high-throughput sequencing data. *Bioinformatics* **31**, 166–169 (2014).
25. Love, M. I., Huber, W. & Anders, S. Moderated estimation of fold change and dispersion for RNA-seq data with DESeq2. *Genome Biol.* **15**, 550 (2014).
26. Modrzynska, K. et al. A knockout screen of ApiAP2 genes reveals networks of interacting transcriptional regulators controlling the *Plasmodium* life cycle. *Cell Host Microbe* **21**, 11–22 (2017).
27. Guerreiro, A. et al. Genome-wide RIP-Chip analysis of translational repressor-bound mRNAs in the *Plasmodium* gametocyte. *Genome Biol.* **15**, 493 (2014).
28. Young, J. A. et al. The *Plasmodium falciparum* sexual development transcriptome: a microarray analysis using ontology-based pattern identification. *Mol. Biochem. Parasitol.* **143**, 67–79 (2005).
29. Bailey, T. L. DREME: motif discovery in transcription factor ChIP-seq data. *Bioinformatics* **27**, 1653–1659 (2011).

Acknowledgements

We thank R. Menard and D. Bargieri for the diCre test plasmid used in this study, and M. Sanders and the WTSI sequencing service for assistance with RNA-seq sample processing. K.K.M. is supported by the Wellcome Trust and the Royal Society (ref. 202600/Z/16/Z). R.S.K. is supported by BBSRC (ref. BB/J013854/1). A.P.W. is supported by the Wellcome Trust (refs 083811 and 107046). O.B. is supported by the Wellcome Trust Sanger Institute (ref. WT098051).

Author contributions

R.S.K. generated and phenotyped HP diCre, diCre test and *PBANKA_0312700* lines, performed phenotyping experiments on the PB_{GAMi} line and generated parasites for transcriptome sequencing. K.K.M. generated the AP2-G overexpression construct and PB_{GAMi} line, performed phenotyping experiments on the PB_{GAMi} line, generated RNA-seq libraries and performed RNA-seq data analysis. R.C. generated 820 diCre and GIMO lines and parasites for transcriptome sequencing. N.P. performed the ookinete conversion assay for *PBANKA_0312700* line. O.B. and A.P.W. led and supervised the study. K.K.M. and A.P.W. wrote the manuscript with contributions from the other authors.

Competing interests

The authors declare no competing interests.

Additional information

Supplementary information is available for this paper at https://doi.org/10.1038/s41564-018-0223-6.

Reprints and permissions information is available at www.nature.com/reprints.

Correspondence and requests for materials should be addressed to K.K.M., O.B. or A.P.W.

Publisher's note: Springer Nature remains neutral with regard to jurisdictional claims in published maps and institutional affiliations.

Corresponding author(s): Katarzyna K Modrzynska, Oliver Billker, Andrew P Waters

Reporting Summary

Nature Research wishes to improve the reproducibility of the work that we publish. This form provides structure for consistency and transparency in reporting. For further information on Nature Research policies, see Authors & Referees and the Editorial Policy Checklist.

Statistical parameters

When statistical analyses are reported, confirm that the following items are present in the relevant location (e.g. figure legend, table legend, main text, or Methods section).

n/a	Confirmed	
☐	☒	The exact sample size (*n*) for each experimental group/condition, given as a discrete number and unit of measurement
☐	☒	An indication of whether measurements were taken from distinct samples or whether the same sample was measured repeatedly
☐	☒	The statistical test(s) used AND whether they are one- or two-sided *Only common tests should be described solely by name; describe more complex techniques in the Methods section.*
☐	☒	A description of all covariates tested
☐	☒	A description of any assumptions or corrections, such as tests of normality and adjustment for multiple comparisons
☐	☒	A full description of the statistics including central tendency (e.g. means) or other basic estimates (e.g. regression coefficient) AND variation (e.g. standard deviation) or associated estimates of uncertainty (e.g. confidence intervals)
☐	☒	For null hypothesis testing, the test statistic (e.g. *F*, *t*, *r*) with confidence intervals, effect sizes, degrees of freedom and *P* value noted *Give P values as exact values whenever suitable.*
☐	☒	For Bayesian analysis, information on the choice of priors and Markov chain Monte Carlo settings
☐	☒	For hierarchical and complex designs, identification of the appropriate level for tests and full reporting of outcomes
☐	☒	Estimates of effect sizes (e.g. Cohen's *d*, Pearson's *r*), indicating how they were calculated
☐	☒	Clearly defined error bars *State explicitly what error bars represent (e.g. SD, SE, CI)*

Our web collection on statistics for biologists may be useful.

Software and code

Policy information about availability of computer code

Data collection	FACS data was collected using FACSDiva Software Version 6.1.3, StepOne™ and StepOnePlus™ Real-Time PCR System software v. 2.1 was used to collect qPCR data
Data analysis	FlowJo (v. 10.3), Samtools (v. 1.3.1), HISAT2 (v 2.0), Integrated Genome Viewer(v. 2.3.91), R studio (v. 1.0.136), Dreme (v. 4.10.0)

For manuscripts utilizing custom algorithms or software that are central to the research but not yet described in published literature, software must be made available to editors/reviewers upon request. We strongly encourage code deposition in a community repository (e.g. GitHub). See the Nature Research guidelines for submitting code & software for further information.

Data

Policy information about availability of data

All manuscripts must include a data availability statement. This statement should provide the following information, where applicable:

- Accession codes, unique identifiers, or web links for publicly available datasets
- A list of figures that have associated raw data
- A description of any restrictions on data availability

RNA-seq data generated in this study is available through GEO database repository (study accession number GSE110201).

Field-specific reporting

Please select the best fit for your research. If you are not sure, read the appropriate sections before making your selection.

☒ Life sciences ☐ Behavioural & social sciences ☐ Ecological, evolutionary & environmental sciences

For a reference copy of the document with all sections, see nature.com/authors/policies/ReportingSummary-flat.pdf

Life sciences study design

All studies must disclose on these points even when the disclosure is negative.

Sample size	For qualitative experiments (i.e genotyping, Western blots) one mouse per strain was used in each of the experiments. For quantitative experiments, the numbers were adjusted based on the variability of the studied trait and the effect size of interest. Thus for quantification of gametocyte production, the means and standard deviations for male and female gametocyte conversion rates were assumed to be 0.028 ±0.011 and 0.033±0.14 respectively based on previous experiments. Therefore (based on the two-sided t-test power calculations in R) n=5 biological replicates were used, as they allow to detect a major (>2 fold) difference in gametocyte production with the significance of < 0.05 with a probability of 0.93 and 0.9 for males and females respectively. Similarly, for the ookinete conversion rate (typically 0.849±0.096), n=3 was chosen as it allows to detect the major difference in the conversion rates (>0.4) with significance of < 0.05 with probability of 0.96. For transcriptome analysis, 6 hour intervals for RNAseq analysis were determined to sufficiently cover the time of gametocyte development without unnecessarily increasing rodent use.
Data exclusions	No Data was excluded from the study.
Replication	Key findings of the manuscript were replicated independently multiple times by two different research teams. Exact number of replicates of each experiment included in figure legends
Randomization	Animals were assigned to experimental groups at random and processed in parallel.
Blinding	All animals/samples were assigned a number and all data was harvested without the knowledge of the infection type or conditions/treatment to ensure minimal bias.

Reporting for specific materials, systems and methods

Materials & experimental systems

n/a	Involved in the study
☒	☐ Unique biological materials
☐	☒ Antibodies
☒	☐ Eukaryotic cell lines
☒	☐ Palaeontology
☐	☒ Animals and other organisms
☒	☐ Human research participants

Methods

n/a	Involved in the study
☒	☐ ChIP-seq
☐	☒ Flow cytometry
☒	☐ MRI-based neuroimaging

Antibodies

Antibodies used	Ter119 PEcy7 (1:500) – Thermofisher, Catalog # 25-5921-81, clone TER-119, lot 4302206, FKBP12 (1:1000) – abcam, Catalog # ab2918, polyclonal, lot GR237896-1 Cre (1:1000) - abcam, Catalog # ab190177, lot GR245386-2 Enolase (1:1000) – rabbit polyclonal antibody generated against Plasmodium berghei α-enolase. Goat Anti-Rabbit IgG-HRP secondary antibody (1:2000)- abcam, Catalog # ab205718, polyclonal, various lots.
Validation	Ter119 PEcy7 (1:500) – Thermofisher, Catalog # 25-5921-81, clone TER-119, lot 4302206, validated by manufacturer for use in flow cytometry in mouse RBC and used in >30 previous publications (https://www.thermofisher.com/antibody/product/TER-119-Antibody-clone-TER-119-Monoclonal/25-5921-81) FKBP12 (1:1000) – abcam, Catalog # ab2918, polyclonal, lot GR237896-1, validated by manufacturer for use in Western blot, can

be blocked with FKBP12 peptide (ab4935) http://www.abcam.com/fkbp12-antibody-ab2918.html, previously used for detection of FKBP12 in closely related apicomplexan parasites: toxoplasma (PMID: 23263690) and Plasmodium falciparum (PMID: 23489321)

Cre (1:1000) - abcam, Catalog # ab190177, lot GR245386-2, validated by manufacturer for use in Western blot, http://www.abcam.com/cre-recombinase-antibody-ab190177.html, previously successfully used for detection of of Cre recombinase in rodents (PMID: 26631266)

Enolase (1:1000) – rabbit polyclonal antibody generated against Plasmodium berghei α-enolase (peptide: KTYDLDFKTPNNDK) by at Proteintech group (Chicago, USA). Used in multiple previous P.berghei publications (PMID: 26118994, PMID: 25275500).

Goat Anti-Rabbit IgG-HRP secondary antibody (1:2000)- abcam, Catalog # ab205718, polyclonal, various lots, validated by manufacturer for use in Western blot, http://www.abcam.com/goat-rabbit-igg-hl-hrp-ab205718.html, used in >50 publications.

Animals and other organisms

Policy information about studies involving animals; ARRIVE guidelines recommended for reporting animal research

Laboratory animals	Female Theiler's Original (TO) (Envigo) 8 -12 weeks of age.
Wild animals	Study did not involve wild animals
Field-collected samples	Study did not involve field samples.

Flow Cytometry

Plots

Confirm that:

☒ The axis labels state the marker and fluorochrome used (e.g. CD4-FITC).

☒ The axis scales are clearly visible. Include numbers along axes only for bottom left plot of group (a 'group' is an analysis of identical markers).

☒ All plots are contour plots with outliers or pseudocolor plots.

☒ A numerical value for number of cells or percentage (with statistics) is provided.

Methodology

Sample preparation	Red blood cells for analysis were collected from tail drops, cardiac puncture or parasite cultures. Cells were suspended in pre-warmed rich PBS with Hoechst 33342 dye and relevant antibodies, and stained for 30 min at 37oC. Stained samples were washed and resuspended in flow cytometry buffer (10% rich PBS, 1 mM EDTA in PBS).
Instrument	SR-II flow cytometer (Becton Dickinson)
Software	FACSDiva Software Version 6.1.3 and FlowJo (v. 10.3),
Cell population abundance	Parasites were typically constituting 1-10% of the total cell population. Gametocytes were between 0.1 and 70% of total parasite population.
Gating strategy	Illustrated and explained in Supplementary Figure S4A

☒ Tick this box to confirm that a figure exemplifying the gating strategy is provided in the Supplementary Information.